JOURNAL OF
EMERGING INVESTIGATORS

Article

Deuterated solvent effects in the kinetics and thermodynamics of keto-enol tautomerization of ETFAA

Aditya Udgaonkar[1,2], Jeslyn Wu[1,3], Aishi Rao[1,3], Edward Njoo[1]

[1] Department of Chemistry, Biochemistry & Physics, Aspiring Scholars Directed Research Program, Fremont, California
[2] BASIS Independent Silicon Valley, San Jose, California
[3] Mission San Jose High School, Fremont, California

SUMMARY

Ethyl 4,4,4-trifluoroacetoacetate (ETFAA) is a β-ketoester that is used as a starting material in the synthesis of a variety of biologically active compounds. The reactivity of this compound is solvent dependent, and here we investigate the kinetics and thermodynamics of keto-enol tautomerization of ETFAA through benchtop 19F NMR in both non-deuterated and deuterated solvents. We determined that tautomerization dynamics in protic and aprotic solvents displayed differences in reaction rates and in the proportion of the keto and enol tautomers present. Moreover, our results demonstrated a positive correlation in aprotic solvents between solvent polarity and the proportion of keto tautomer present. We further employed density functional theory (DFT) calculations to probe the specific chemical interactions responsible for these observed trends. From the DFT calculations it was found that the major source of stability of the enol tautomer compared to the keto tautomer was its intramolecular hydrogen bond. Knowing the equilibrium of the keto-enol tautomerization of ETFAA is vital for synthesis of biologically active compounds derived from ETFAA, and maintaining a computational perspective can be useful in determining the advantages and disadvantages of various computational methods used in modeling keto-enol tautomerization.

INTRODUCTION

Fluorinated small molecules make up 20% of all small molecule drugs approved for clinical use and have thus captured the attention of chemists and clinicians alike (1). Moreover, trifluoromethylated small molecules make up over 19% of fluorinated chemical entities (1-3). The advantage of fluorinated molecules in clinical use is that they possess improved metabolic stability, better absorption by cells, and increased binding affinities (4). Ethyl 4,4,4-trifluoroacetoacetate (ETFAA), a β-ketoester with broad synthetic utility in medicinal chemistry, is a starting material in the synthesis of a variety of trifluoromethylated small molecules with biological significance. These include the quinolin-2(1H) skeleton (5) and novel 2-(1,2,3-triazolylmethoxy) and isoxazole tagged 2H-chromene derivatives (6), which have been demonstrated to possess anti-cancer and cytotoxic properties (**Figure 1**). Numerous compounds have been synthesized starting from ETFAA that also possess antibacterial and antifungal activity, including pyrazole carboxamides (7), isoxazoles (8), 4-amino-2-phenylindole-based compounds (9), and 1, 2, 4-oxadiazole and (1*H*-pyrazol-4-yl)-methanone oxime derivatives (8). Moreover, ETFAA has been utilized in many reported multicomponent reactions, such as the Biginelli cyclocondensation reaction, which allow for the rapid and combinatorial generation of large compound libraries (10, 11). For example, trifluoromethyl-substituted hexahydropyrimidines (10), which demonstrated antibacterial activity, and fluorinated condensed pyrano-pyrazoles (11), which displayed selective cytotoxicity against cancer cells,

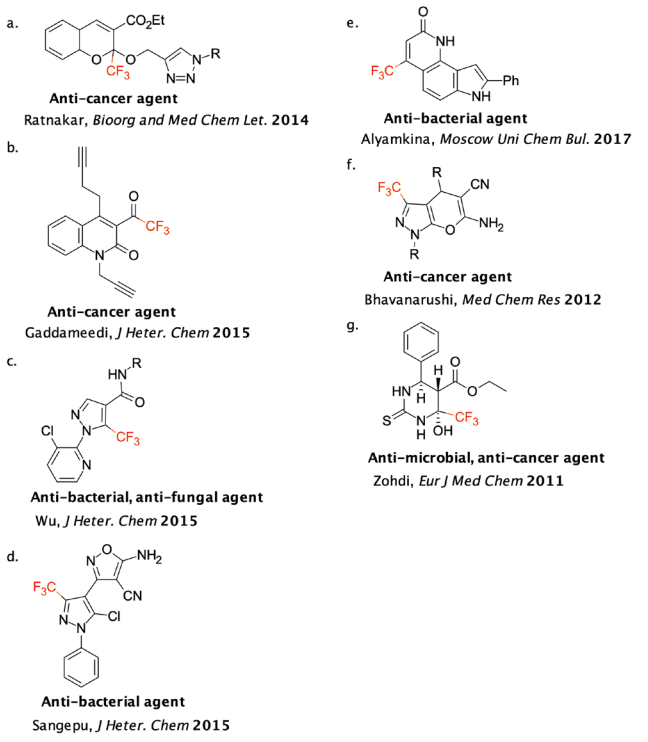

Figure 1: Examples of synthetic biologically active compounds that utilize ETFAA as a starting material. Compounds 1a (6), 1b (5), 1c (7), which are a 1,2,3-triazole functionalized 2H-Chromene derivative, a quinolin-2(1H)-one derivative, and a pyrazole carboxamide derivative, respectively, all display cytotoxic abilities. Compounds 1d (8), 1e (9), 1f (11), 1g (10), which are a novel isoxazole derivative, a 4-amino-2-phenylindole-based derivative, a pyrano pyrazole derivative, and a trifluoromethyl-substituted hexahydropyrimidine, respectively, all possess antibacterial or antifungal activity. The -CF3 moiety, originated from ETFAA, of each biologically active compound is highlighted in red.

are both synthesized by one-pot multicomponent reactions involving ETFAA.

Ketones and other carbonyl-containing compounds, such as ETFAA, with acidic α-protons often exist in equilibrium between *keto* and *enol* tautomers in solution (**Figure 2**). The keto tautomer possesses a carbon-oxygen double bond, known as a keto group, and the enol tautomer possesses an alcohol group adjacent to a carbon-carbon double bond. Several studies have shown that the solvent environment plays a major role in the equilibrium between these two tautomers (12-15). Understanding the equilibrium of tautomerization provides insights into the reactivity of ETFAA and facilitates the synthesis of such trifluorinated biologically active compounds. Previous studies have suggested that polar and protic solvents, i.e., solvents with a hydrogen connected to an electronegative element such as oxygen, nitrogen, or fluorine, stabilize the greater dipole moment in the ketone tautomer and also disrupt the intramolecular hydrogen bonding network present in the enol tautomer (12, 13). In contrast, nonpolar and aprotic solvents, solvents with hydrogens not connected to an electronegative element, tend to allow the enol to exist as the favored tautomer due to stability conferred by the 6-membered intramolecular hydrogen bond (12, 13). Researchers have previously determined the equilibrium constants of the keto-enol tautomerization of ETFAA by

Figure 2: Structures and dipole moments of the enol and keto tautomers of ETFAA. a) ETFAA exists in equilibrium between keto and enol tautomers, and the relative quantities of these two tautomers present at equilibrium is dependent on the solvent environment. The trifluoro group is a region of high electron density and partial negative charge (δ-). The carbon atom adjacent to the trifluoro group in the keto and enol tautomers bears a partial positive charge (δ+) due to resonance and electron withdrawing effects from the trifluoro group.

proton nuclear magnetic resonance spectroscopy (^{1}H NMR) under deuterated chloroform and dimethyl sulfoxide (12, 13). Additionally, the reactivity and chemical behavior of ETFAA and other β-ketoesters are also solvent dependent (12-15); this can be partly attributed to relative concentrations of keto and enol tautomers present in solution at equilibrium. However, the requirement for deuterium to lock high field NMR spectrometers has previously limited the study of keto-enol tautomerization of ETFAA to deuterated solvents, whose cost can become prohibitive in running reactions on a large scale. Non-deuterium lock options on benchtop spectrometers have circumvented this limitation (16).

Here, we utilize benchtop ^{19}F NMR, a smaller and more compact instrument than regular ^{1}H NMR, to conveniently track keto-enol equilibration in real-time in both deuterated and non-deuterated solvents as a means of determining solvent effects in both the kinetics and thermodynamics of keto-enol equilibrium. Moreover, we report the thermodynamics and kinetic isotope effects of the keto-enol tautomerization of this compound in both deuterated and non-deuterated solvents using the trifluoromethyl group (-CF_3) as a handle for reaction monitoring by benchtop ^{19}F NMR demonstrated in **Figure 3**. The use of ^{19}F NMR is not limited to deuterated solvents because of its ability to utilize either ^{2}H or ^{1}H as a lock nucleus (16, 17), a method to control magnetic fields in the NMR sample to prevent the drift of resonance frequencies.

We hypothesize that, in protic and polar aprotic solvents with hydrogen bond acceptor capabilities, the keto tautomer of ETFAA will be favored due to the disruption of the intramolecular hydrogen bond of the enol tautomer (14, 15). In addition, we predict that the solvent effects between deuterated and non-deuterated solvents on the keto-enol tautomerization of ETFAA will be greater in protic solvents such as methanol because of kinetic isotope effects resulting from differences in O-H versus O-D bond breakage events where the solvent plays an explicit role in the proton transfer steps of tautomerization (18). We supported our experimental approach with density functional theory (DFT)

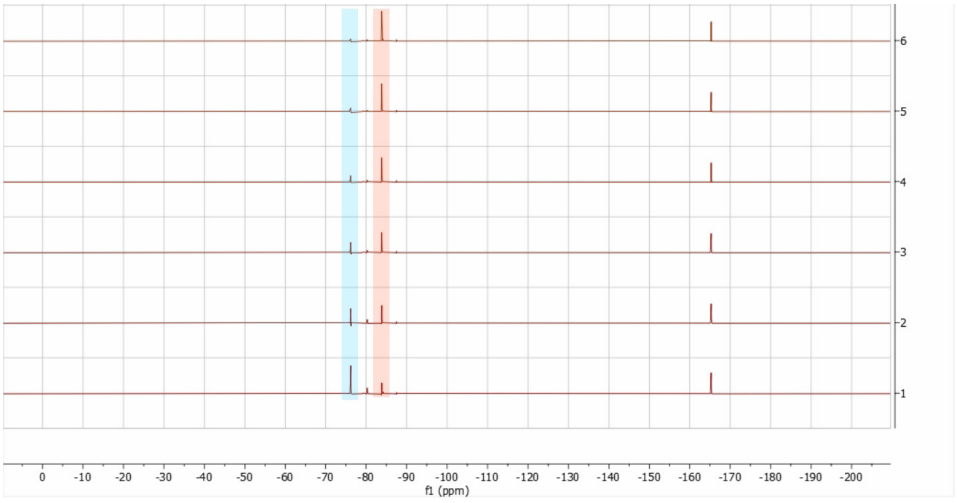

Figure 3: NMR time course experiment for methanol. "f1" on the x-axis represents the chemical shifts, and there are six timestamps spaced apart by an average of sixteen seconds, represented on the y-axis. The resonance at δ = -76.16 ppm, shaded in blue, which gradually decreases in intensity as a function of time, corresponds to the enol tautomer, and the resonance at δ = -83.97 ppm, shaded in red, which gradually increases in intensity as a function of time, corresponds to the keto tautomer (14). The resonance at δ = -165.39 ppm corresponds to the internal standard, hexafluorobenzene (C_6F_6).

to see if different functionals and basis sets accurately predict the thermodynamics and kinetic isotope effects of the tautomerization.

Examination of our data revealed the existence of kinetic isotope effects between deuterated and non-deuterated methanol and a positive correlation between solvent polarity and favorability of the keto tautomer. However, the DFT calculations vastly overestimated the stability of the enol tautomer, thus highlighting shortcomings of the continuum solvation model (CPCM) in modeling chemical interactions with respect to hydrogen bonding. Understanding the equilibrium of the tautomerization of ETFAA can aid in the synthesis of trifluoronated, biologically active compounds derived from ETFAA, and taking a computational approach can give insight into the strengths and weaknesses of different models, functionals, and basis sets in computationally modeling the keto-enol tautomerization of β-keto esters.

RESULTS

The concentrations of the enol and keto tautomers over time were determined by quantitative NMR and used to calculate the rate and equilibrium constants of tautomerization. DFT calculations using the 6-31G and def2-SVP basis sets and the LDA, B3LYP, BLYP, and M06L functionals were done to calculate the Gibbs Free Energy change (ΔG) of the tautomerization reaction and bond frequencies of the O-H and O-D bonds of methanol and deuterated methanol, which involved eight basis set-functional combinations for methanol and deuterated methanol each.

Kinetics

It is observed that the enol concentration over time decreases, whereas the keto concentration over time increases (**Figure 3, 4A**). Under an experiment using deuterated methanol, the enol concentration decreases from 0.123 M to 0.0175 M and the keto concentration increases from 0.072 M to 0.2 M (**Figure 4A**). After analyzing the NMR data and determining the concentrations over time, we observed different kinetic behavior for the tautomerization of ETFAA between methanol (a protic solvent) and the aprotic solvents. We observed that the equilibration of enol to keto tautomers of ETFAA is described by first order kinetics in both deuterated and non-deuterated methanol with rate constant values of 0.005537 s^{-1} and 0.02564 s^{-1}, respectively, corresponding to an experimental kinetic isotope effect (KIE) of 4.63. The rate constants were determined by taking the negative of the slope of the natural log of the enol concentration over time (**Figure 4B**). The KIE was the ratio of the rate constants of tautomerization in non-deuterated methanol over deuterated methanol, thus highlighting the difference in the rates. Similarly, theoretical KIE values were derived using Equation [1] from differences in the O-H and O-D bond vibrational energies, & respectively, computed at various levels of theory (**Figure 4C**). Among the different basis sets and functional combinations, the theoretical KIE values ranged from 9.63 to 11.81 whereas the experimental KIE value was smaller at a value of 4.63.

$$ln(\frac{k_h}{k_d}) = \frac{(-\frac{1}{2})hc(\underline{u_H}-\underline{u_D})}{KT} \quad [1]$$

Here, k_h/k_d represents the rate constant ratio of tautomerization in protonated methanol over deuterated methanol, *h* is Planck's constant (J•K), *c* is the speed of light (m/s), *K* is the Boltzmann constant (*J*/*K*), *T* is the temperature in Kelvin, and *uH* & *uD* are the wavenumbers for the C-H and C-D bond stretch, respectively (cm^{-1}).

Interestingly, we observed that the reaction kinetics of the tautomerization in aprotic solvents and their deuterated counterparts did not linearize in the 0th, 0.5th, 1st, 1.5th, and 2nd orders, to account for the possibility of different mechanistic pathways. Among the various aprotic solvents, the average rates of the decrease of the enol concentration ranged from 0.00003 to 0.0000593 M/s (**Figure 4D**). This was found by taking the slope of the linear regression line modeling the enol concentration over time. The differences in the kinetics of equilibration between the deuterated and non-

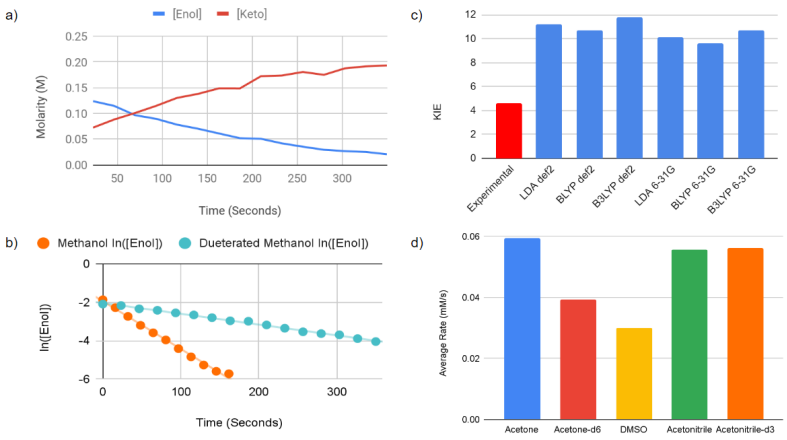

Figure 4: Kinetic data of the tautomerization of ETFAA. a) Concentrations of the enol (blue) and keto (red) species under a time course experiment in deuterated methanol. The concentrations were determined through quantitative ^{19}F NMR, using a hexafluorobenzene internal standard. b) Natural logarithm of the enol concentration over time in methanol and deuterated methanol. A line of best fit is shown for each. c) Experimental and computational kinetic isotope effects (KIE) for the methanol species. The bond frequencies were calculated using two basis sets, def2-SVP and 6-31G, and three functionals, B3LYP, BLYP, and LDA. Since DFT uses a pure solvent system with no impurities, the true KIE can be determined. d) Bar graph of the average rate of the decrease in the enol concentration, among the various aprotic solvents. No decrease in the enol concentration was observed under chloroform, deuterated chloroform, and deuterated dimethyl sulfoxide.

deuterated solvents were small in these solvents. Acetone, an aprotic solvent, does not linearize when the natural log of the enol concentration is graphed with respect to time, whereas in methanol the tautomerization reaction is first order and displays faster conversion to the keto tautomer from the enol tautomer (**Figure 5A**).

Equilibrium and Thermodynamics

We observed that the keto-enol tautomerization in methanol strongly favored the keto form, whereas the enol form tended to exhibit a higher concentration in aprotic solvents, according to the experimental changes in ΔG, where equilibrium is defined as K = [*Keto*]/[*Enol*] (**Figure 5B**). A positive correlation was found between dielectric and equilibrium constants among aprotic solvents (**Figure 5C**). This correlation was notably stronger upon the removal of deuterated acetonitrile, which acted as the sole outlier.

When the ΔG of the tautomerization reaction was calculated from self-consistent field (SCF) energy values derived from the outputs of the DFT optimization, it was found that these free energy changes are much larger than those observed in our ^{19}F NMR experiments, suggesting that DFT as a whole overestimates the stability of the enol tautomer (**Figure 6A**). With both the def2-SVP and 6-31G basis sets, the LDA (local density approximation) functional exhibited the greatest overestimation of ΔG whereas the

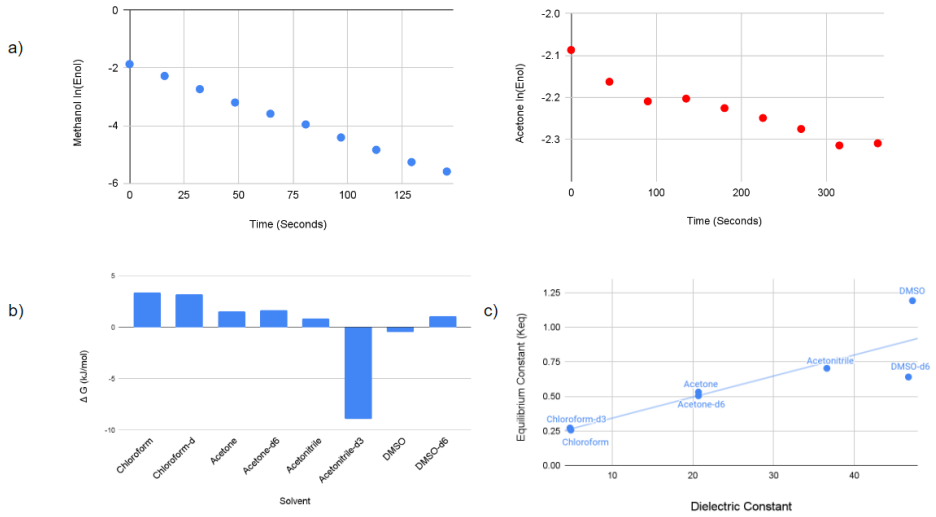

Figure 5: The effect of solvent polarity on the kinetics and thermodynamics of the tautomerization of ETFAA. a) Graph of the natural logarithm of the enol concentration versus time in methanol (blue) and acetone (red). b) Experimental change in Gibbs free energy (ΔG) for aprotic solvents. c) Scatterplot between the equilibrium constants (K_{eq}) and the dielectric constants of the solvents, without the deuterated acetonitrile outlier.

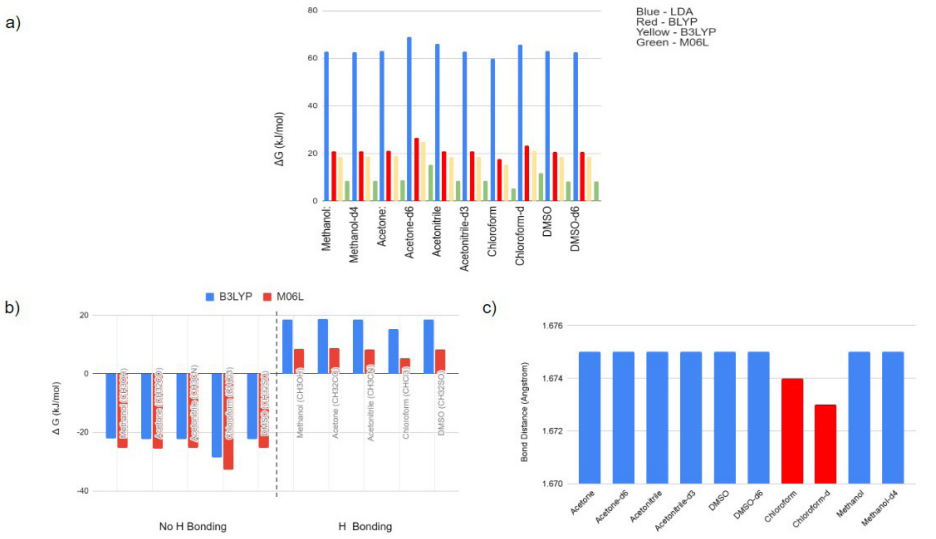

Figure 6: Computational calculations relating to the thermodynamics of the tautomerization of ETFAA. a) Change in Gibbs free energy (ΔG) in different solvents with the def2-SVP basis set and four functionals of LDA, B3LYP, BLYP, and M06L. b) The change in ΔG with and without the intramolecular hydrogen bond in the enol. When removing the intramolecular hydrogen bonding effect, there is a decrease in ΔG, indicating favorability of the keto form. c) The predicted bond length in angstroms of the intramolecular hydrogen bond in the enol tautomer. The predicted O-H hydrogen bond distance of ETFAA, where the solvent is treated implicitly, is 1.675 A, except in chloroform. The O-H hydrogen bond distances of ETFAA in chloroform and deuterated chloroform are 1.674 Å and 1.673 Å, respectively.

Minnesota 2006 local functional (M06L) gave values closest to our experimental results. As predicted across the 10 different solvents, the predicted free energy changes of the tautomerization reaction were similar in value between functionals regardless of the varying basis sets (**Figure 6A**). In order to probe whether this over-estimation of enol stability might be related to the predicted strength of the intramolecular hydrogen bonding network, free energy changes were again calculated in the absence of the enol O-H proton, and when this was done, the free energy difference ended up favoring the keto tautomer (**Figure 6B**). Moreover, through Avogadro, the hydrogen bond distances were calculated and under all solvents except for chloroform and deuterated chloroform the hydrogen bond length of the enol was 1.675 Angstroms (**Figure 6C**).

Upon observation, our experimental data revealed the existence of kinetic isotope effects on the tautomerization of ETFAA when comparing the rate of tautomerization between methanol and deuterated methanol. Moreover, we showed that there exists a positive correlation between the dielectric constant or polarity of a solvent and a higher proportion of the keto tautomer in equilibrium. When computationally modeling equilibrium, our DFT calculations vastly overestimated the favorability of the enol tautomer.

The rate of keto-enol tautomerization of ETFAA demonstrated a defined kinetic isotope effect in methanol because the -O-H/O-D bond is able to participate more in heterolytic bond cleavage events (18). The experimental kinetic isotope effect of the keto-enol tautomerization in methanol was 4.632, but through DFT the theoretical KIE ranged from 9.63 to 11.81, among the different basis sets and functional combinations. We believe that the computational KIE is higher because DFT models a pure solvent system without impurities that increase the rate of tautomerization in deuterated methanol. In reality, deuterated methanol is hygroscopic and likely contains residual water.

However, because the -C-H/C-D bond is unable to participate in proton transfer events, there is no observed kinetic isotope effect when the reaction is performed in aprotic solvents. Moreover, in aprotic solvents, the kinetics do not fit with the reaction orders of 0, 0.5, 1, 1.5, and 2. One explanation is that the tautomerization from the enol to the keto form involves different and simultaneous proton transfer mechanisms. One plausible mechanism is that both the enol tautomers react with each other (**Figure 7A**). Another plausible mechanism is that the solvent may catalyze the conversion of the enol to the keto form by acting as an acid or base. Lastly, trace impurities of water may participate in a concerted mechanism with the enol to yield the keto form (**Figure 7B**) (19). These simultaneous reaction pathways may have resulted in the data for the aprotic solvents not conforming to a specific reaction order. A Karl-Fischer titration could be done to test the water content in the aprotic solvents to determine its role in affecting the reaction orders.

The tautomerization in methanol possesses the highest Keq because the protic -O-H bonds are able to have competitive hydrogen bonding with the enol (14, 15). Our putative explanation is that hydrogen bonding engagements between the substrate and the solvent cage disrupt the intramolecular hydrogen bonding network of the enol, thus favoring the keto form (20). Moreover, the positive correlation of the dielectric constants of the aprotic solvents and

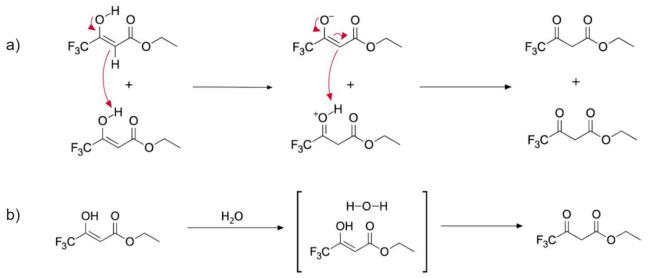

Figure 7: Plausible additional tautomerization mechanisms of ETFAA. a) Intermolecular tautomerization mechanism of ETFAA. b) Water concerted tautomerization mechanism.

equilibrium constants suggests that polarity of the solvent is important in stabilizing the keto tautomer, which has a greater dipole moment of 2.649 debye than the enol tautomer which has a dipole moment of 1.218 debye (21). The dipole moment values were taken from Avogadro.

The difference between the experimental and computational free energy changes could be explained by the fact that DFT overestimates the stability of the intramolecular hydrogen bond. When the intramolecular hydrogen bonding effects were removed, the ΔG values fell, indicating that the keto form is more favored. Moreover, when modeling the hydrogen bond distances using Avogadro, the bond distances were relatively constant, which suggests that in an implicit solvation model the DFT and the quantum mechanics approach most likely overestimate hydrogen bond strength in protic solvents because it fails to account for hydrogen bonding events between the solvent and substrate that would disrupt such an intramolecular hydrogen bond. This demonstrates a limitation in modeling tautomerization computationally: an implicit solvation model such as CPCM being used to account for explicit chemical interactions and hydrogen bonding competition between substrate and solvent cage. Among the different functionals LDA, BLYP, B3LYP, and M06L, LDA performed the worst in accurately modeling the tautomerization equilibrium of ETFAA and M06L performed the best. This is due to LDA assuming a constant electron density throughout the molecule, whereas BLYP, B3LYP, and M06L take into account non-uniform electron density (22, 23). On a polar molecule such as ETFAA, the electron density fluctuates because of the electronegative trifluoro group.

^{19}F benchtop NMR provides a fast and convenient method for monitoring reactions in real time. Here, we demonstrate an example of its use in monitoring the keto-enol tautomerization of ETFAA. Using quantitative NMR, we were able to deduce the molarities of the tautomer species over time and calculate rate and equilibrium constants to attain mechanistic insights into solvent effects in tautomer equilibration. This monitoring can be used to measure keto-enol tautomerization across many fluorinated molecules and could be extended to other NMR active nuclei such as 29Si; further work on applying this platform for real-time reaction monitoring in the synthesis of trifluoromethylated small molecules from ETFAA is currently underway.

MATERIALS AND METHODS

Experimental

The rate constants and equilibrium constants of each

tautomerization reaction were determined by quantitative ^{19}F NMR in monitoring changing concentrations of keto and enol tautomers of ETFAA with spectroscopic grade hexafluorobenzene (C_6F_6) as an internal standard. NMR spectra were acquired on an Nanalysis NMReady 60PRO through ^{19}F NMR (56 MHz). Each kinetic experiment had a 30 second tau. The concentrations of each tautomer were determined over time by integration against the internal standard. The order of the reaction was then determined by finding a linear best fit under the integral rate laws for 0th, 0.5th, 1st, 1.5th, and 2nd order. After finding the respective integrated rate law, we then used the slope to find the rate constant or average rate for each solvent. Each reaction was performed in triplicate, each containing hexafluorobenzene at a 0.02 M scale and ETFAA at a 0.10 M scale, in five non-deuterated solvents (methanol, acetonitrile, dimethyl sulfoxide, chloroform, and acetone) and their deuterated counterparts.

All solvents and reagents were procured from commercially available sources and used without additional purification. Methanol (HPLC grade) was acquired from Concord Technology. Acetone (99.8+%) was acquired from Acros Organics. Acetonitrile (99.5%) was acquired from Carolina Chemical. Chloroform (99.8%), deuterated chloroform (99.8%), and deuterated acetonitrile (99.8%) were acquired from Beantown Chemical. DMSO (99.995%) was acquired from DMSO Store. Deuterated methanol (99.8%) was acquired from Cambridge Isotope Laboratories. D6-acetone (>99% purity, >99.8% 2H) was acquired from Martek Isotopes. Deuterated DMSO (99.8%) was purchased from Millipore Sigma. Ethyl 4,4,4-trifluoroacetoacetate (95%) was acquired from AK Scientific and was used without further purification. Spectroscopic grade hexafluorobenzene (>99%) was purchased from Sigma Aldrich.

To find the equilibrium constants, samples were allowed to equilibrate in solution at room temperature over the course of two days, and relative concentrations of the keto and enol tautomers and the internal standard were determined by quantitative ^{19}F NMR. All NMR spectra were processed using MestreNova software. The equilibrium constant is defined as K_{eq} = [*Keto*]/[*Enol*], where the enol tautomer is the reactant and the keto form is the product. The enol tautomer was chosen as the reactant because ETFAA exists with a high concentration of enol, and in most cases the concentration of the enol form was found to decrease over time, whereas the concentration of the keto tautomer increased over time. Each entry was performed in triplicate.

Computational

Using molecular mechanics and force fields, geometry optimizations of 10,000 steps were performed on the keto and enol tautomers of ETFAA using Avogadro (21). For the DFT calculations, we used two basis sets (6-31G and def2-SVP), four functionals (LDA, B3LYP, BLYP, and M06L), and the CPCM in our five non-deuterated and corresponding deuterated solvents. The two basis sets and four functionals were chosen because of their common use and less intensive computational methods. All DFT calculations were performed on a Dell PowerEdge 710 server cluster with a 24-core Intel Xeon X5660 processor at 2.80 GHz and 32 GB RAM.

Using these computational methods, we then performed single point energy calculations on each keto and enol structure. Using the final calculated single point energies for both tautomeric forms, we calculated ΔG for each reaction by finding the difference in SCF energy between the keto and enol species to approximate the enthalpy change of tautomerization (ΔH). We ignored the entropy change (ΔS) as it was negligible (15). The change in Gibbs' free energy was then calculated by determining the enthalpy of the reaction and using Equation [2]. Using ΔG values, the equilibrium constant (K) for each tautomerization reaction was calculated by Equation [3].

$$\Delta G = \Delta H \quad [2]$$

$$\Delta G = -RTln(K) \quad [3]$$

To determine the bond frequencies of the O-H and O-D bonds to calculate the computational kinetic isotope effects, geometry optimizations of 10,000 steps were performed on methanol and deuterated methanol using Avogadro. The bond frequency calculations were subsequently performed on ORCA, with the def2-SVP and 6-31G basis sets and the LDA, BLYP, and B3LYP functionals. The CPCM model was used to capture the solvent dielectric. The dielectric constants were taken from the Merck Index (24).

Received: June 15, 2021
Accepted: February 25, 2022
Published: December 2, 2022

REFERENCES

1. Inoue, M., *et al*. "Contribution of Organofluorine Compounds to Pharmaceuticals." *ACS Omega*, vol. 5, no. 19, Apr. 2020, doi:10.1021/acsomega.0c00830.
2. Yale, H. L. "The trifluoromethyl group in medical chemistry." *Journal of Medicinal Chemistry*, vol. 1, no. 2, Apr. 1959, pp. 121-133. doi:10.1021/jm50003a001.
3. Kiselyov, A. S., *et al*. "The trifluoromethyl group in organic synthesis. a review." *Organic preparations and procedures international,* vol. 28, no. 9, Jun. 1996, pp. 289-318. doi:10.1080/00304949609356536.
4. Shah, P., *et al*. "The role of fluorine in medicinal chemistry." *Journal of Enzyme Inhibition and Medicinal Chemistry,* vol. 22, no. 5, Jan. 2007, doi: 10.1080/14756360701425014.
5. Gaddameedi, J. D., *et al*. "Synthesis and Anticancer Activity of Novel N-trisazole/isoxazole Alkyl Functionalized Quinolin-2(1H)-one Derivatives." *Journal of Heterocyclic Chemistry,* vol. 54, no. 1, Dec. 2015, pp. 194-205. doi:10.1002/jhet.2566.
6. Ratnakar Reddy, K., *et al*. "Synthesis of novel 1,2,3-triazole/isoxazole functionalized 2H-Chromene derivatives and their cytotoxic activity." *Bioorganic & Medicinal Chemistry Letters,* vol. 24, no. 7, Apr. 2014, pp. 1661-1663. doi:10.1016/j.bmcl.2014.02.069.
7. Wu, Z., *et al*. "Synthesis and Bioactivities of Novel1-(3-Chloropyridin-2-yl)-N-Substituted-5-(Trifluoromethyl)-Pyrazole Carboxamide Derivatives." *Journal of Heterocyclic Chemistry,* vol. 54, no. 1, Dec. 2015, pp. 325-330. doi:10.1002/jhet.2587.
8. Sangepu, B., *et al*. "Synthesis of Isoxazole, 1, 2, 4-Oxadiazole and (1H-Pyrazol-4-yl)-methanone Oxime Derivatives from N-Hydroxy-1H-pyrazole-4-carbimidoyl Chloride and their Biological Activity." *Journal of Heterocyclic Chemistry,* vol. 53, no. 3, May. 2015, pp.

754-761. doi:10.1002/jhet.2309.
9. Alyamkina, E. A., *et al*. "4-amino-2-phenylindole-based compounds with potential antibacterial activity." *Moscow University Chemistry Bulletin,* vol. 72, no. 1, Apr. 2017, pp. 24-28. doi:10.3103/s0027131417010023.
10. Zohdi, H. F., *et al*. "Green synthesis and antimicrobial evaluation of some new trifluoromethyl-substituted hexahydropyrimidines by grinding." *European Journal of Medicinal Chemistry,* vol. 46, no. 11, Nov. 2011, pp. 5636-5640. doi:10.1016/j.ejmech.2011.09.036.
11. Bhavanarushi, S., *et al*. "Synthesis, cytotoxic, and DNA binding studies of novel fluorinated condensed pyrano pyrazoles." *Medicinal Chemistry Research,* vol. 22, no. 5, Sep. 2012, pp. 2446-2454, doi:10.1007/s00044-012-0239-z.
12. Cook, A. G., *et al*. "Determination of Solvent Effects on Keto—Enol Equilibria of 1,3-Dicarbonyl Compounds Using NMR." *Journal of Chemical Education,* vol. 84, no. 11, Nov. 2007, pp. 1827, doi:10.1021/ed084p1827.
13. Cook, A. G., *et al*. "Correction to Determination of Solvent Effects on Keto-Enol Equilibria of 1,3-Dicarbonyl Compounds Using NMR." *Journal of Chemical Education,* vol. 87, no. 7, May. 2010, pp. 678-679. doi:10.1021/ed1000813.
14. Sloop, *et al*. "Keto–enol and enol–enol tautomerism in trifluoromethyl-β-diketones." *Journal of Fluorine Chemistry,* vol. 127, no. 6, Jun. 2006, pp. 780-786. doi:10.1016/j.jfluchem.2006.02.012.
15. Charif, *et al*. "Solvent effects on the keto-enol tautomeric equilibrium of tetronic and ethyl acetoacetate carbon acids: A theoretical study." *Journal of Theoretical and Computational Chemistry*, vol. 9, no. 6, May. 2010, pp 1021-1032. doi:10.1142/s0219633610006171.
16. Beek, T. A. "Low-field benchtop NMR spectroscopy: status and prospects in natural product analysis." *Phytochemical Analysis.* vol. 32, no. 1, Jan. 2020, doi:10.1002/pca.2921.
17. Danieli, E., *et al*. "On-Line Monitoring of Chemical Reactions by using Bench-Top Nuclear Magnetic Resonance Spectroscopy." *ChemPhysChem.* vol. 15, no.14, Aug. 2014, pp. 3060-3066. doi:10.1002/cphc.201402049.
18. P. B. Armentrout, *et al*. "Understanding heterolytic bond cleavage." *Journal of the American Chemical Society,* vol. 114, no. 22, Oct. 1992, pp. 8627-8633, doi: 10.1021/ja00048a042.
19. Wirz, J, "Kinetic studies of Keto–Enol and other tautomeric equilibria by flash photolysis." *Advances in Physical Organic Chemistry - Advan Phys Organ Chem.* vol. 44, Dec. 2010, pp. 325-356. doi:10.1016/S0065-3160(08)44006-6.
20. Nagy, P. "Competing Intramolecular vs. Intermolecular Hydrogen Bonds in Solution." *International Journal of Molecular Sciences,* vol. 15, no. 11, Oct. 2014, pp. 19562-19633, doi:10.3390/ijms151119562.
21. Avogadro: An Open-Source Molecular Builder and Visualization Tool, version 1.2.
22. Chan, B., *et al*. "Performance of Gradient-Corrected and Hybrid Density Functional Theory: Role of the Underlying Local Density Approximation and the Gradient Correction." *Journal of Chemical Theory and Computation*, vol. 8, no. 12, pp. 4899-4906, doi:10.1021/ct300603d.
23. Wang, Y., *et al*. "Revised M06-L functional for improved accuracy on chemical reaction barrier heights, noncovalent interactions, and solid-state physics." *Proceedings of the National Academy of Sciences,* vol. 114, no. 32, pp. 8487-8492. doi:10.1073/pnas.1705670114.
24. O'Neil M.J., *et al*. "The Merck Index: An Encyclopedia of Chemicals, Drugs, and Biologicals, Fourteenth Edition." *Journal of Chemical Information and Modelling,* vol. 47, no. 2, Mar. 2007, doi:10.1021/ci700022n.